Supplementary Information for

A brain-enriched lncRNA shields cancer cells from immune-mediated killing for metastatic colonization in the brain

Weiguang Liu[1#], Peng Sun[2#], Lingling Xia[1], Xilin He[1], Zhengmiao Xia[1], Yehong Huang[1], Wenzhuo Liu[1], Lulu Li[1], Liming Chen[1, 3*]

[1]Department of Biochemistry, School of Life Sciences, Nanjing Normal University, Nanjing, China
[2]State Key Laboratory of Oncology in South China, Collaborative Innovation Center for Cancer Medicine, Department of Pathology, Sun Yat-sen University Cancer Center, Guangzhou, China
[3]Cancer Institute, School of Life Sciences, Nanjing Normal University, Nanjing, China
[#]W. L. and P.S. contributed equally to this work
[*] Corresponding author: Liming Chen;
Email: chenliming1981@njnu.edu.cn

This PDF file includes:

Captions for figures
Figures S1 to S7
Tables S1 to S3
Legends for Datasets S1 to S6

Other supplementary materials for this manuscript include the following:

Datasets S1 to S6

Supplementary Information Text

Additional procedures

RT–qPCR analysis. All experiments were carried out by following the manufacturers' instructions. In brief, RNAs were reverse-transcribed into cDNA using HiScript II Q-RT SuperMix (Vazyme), and qPCR was performed using ChamQ SYBR Qpcr Master Mix (Vazyme). The relative expression levels of lncRNAs and mRNAs were calculated according to the $2^{-\Delta\Delta Ct}$ method. GAPDH served as the internal control. Primer sequences for RT**–**qPCR are listed in Table S1.

Subcellular fractionation. In brief, cells were collected by trypsinization and washed with 1 × PBS buffer three times. Then, the cells were lysed with lysis buffer A (10 mM HEPES solution, 10 mM KCl, 2 mM $MgAc_2$, 3 mM $CaCl_2$, 340 mM sucrose, 1 mM dithiothreitol, 1 mM PMSF, 0.25% NP-40, pH 7.9) and incubated on ice for 30 min. The cell lysate was centrifuged to collect the supernatant as the cellular cytoplasmic fraction. The remaining cell pellet was resuspended in lysis buffer B (50 mM HEPES, 500 mM NaCl, 1.5 mM $MgCl_2$, 0.1% Triton-X100, 1 mM DTT, pH 7.9) and incubated on ice for 30 min. Then, the sample was centrifuged to collect the supernatant as the cellular nucleic fraction. BMOR, U6 and GAPDH levels were examined by RT–qPCR, where U6 and GAPDH served as markers for the cytoplasmic and nucleic fractions, respectively.

5' and 3' rapid amplification of cDNA ends (RACE). We performed 5' and 3' RACE using the SMARTer RACE 5'/3' Kit (Takara) following the manufacturer's protocol. The RACE PCR fragments were sequenced using Sanger sequencing. The primers used are listed in Table S2.

In vitro transcription/translation. In vitro transcription/translation experiments were performed following the protocols provided by the manufacturers. Briefly, T7 promoter containing DNA sequences or plasmids was used in a TNT® Quick Coupled Transcription/Translation System (Promega). Then, 1 μg plasmid DNA template was mixed with 40 μl TNT® T7 Quick Master Mix, 1 μl methionine (1 mM), 1 μl Transcend™ Biotin-Lysyl-tRNA, and nuclease-free water for a final volume of 50 μl per reaction. The reaction tube was incubated at 30 ℃ for 90 min, and 1 μl reaction product was added into diluted 2 × SDS loading sample buffer for immunoblot analysis by detecting the signals using streptavidin-HRP (Cell Signaling Technology).

Cell transfection and lentiviral infection. Plasmids used in cell transfection and lentiviral infection were constructed according to standard protocols. Related primer sequences are shown in Table S3. For cell transfection, we used Lipofectamine 2000 reagent (Invitrogen) according to the manufacturer's protocol. For lentiviral infection, first, lentiviral particles were produced. In brief, 5 × 10^6 HEK293T cells were seeded for 24 h and then cotransfected with 4 μg shRNA expression vector (pLKO.1-shRNA control or pLKO.1-BMOR-shRNA#1 or pLKO.1-BMOR shRNA#2), 3 μg pSPAX2 and 1 μg pMD2. G plasmid using Lipofectamine 2000 reagent according to the manufacturer's instructions. Then, lentiviral particles were produced and collected for lentiviral infection.

Migration and invasion assays. Migration and invasion assays were performed using Transwell migration chambers (Merck Millipore) following the manufacture's protocol. In brief, 2 × 10^5 cells were seeded with serum-free DMEM into the upper chamber, and 600 μl 20% FBS DMEM was placed in the lower chamber. The chamber was incubated for 36 h in a humidified incubator with an atmosphere of 5% CO_2 at 37 ℃. Then, the cells were fixed with 4% paraformaldehyde and stained with 0.1% crystal violet.

LDH cytotoxicity assays. Cell cytotoxicity was detected through LDH release using an LDH Cytotoxicity Assay Kit (Beyotime) according to the manufacturer's protocol. In brief, cells were seeded in a 96-well plate with or without 2 μg/ml poly(I:C) treatment. After incubation for 24 h, the cell culture media was collected, and dead cell debris was removed via centrifugation. Then, the supernatants were transferred to a new 96-well plate and pulsed with LDH release reagent. The mixtures were incubated in a cell incubator for 1 h. LDH release was detected by measuring the absorbance at 490 nm using a Bio–Rad iMark plate reader.

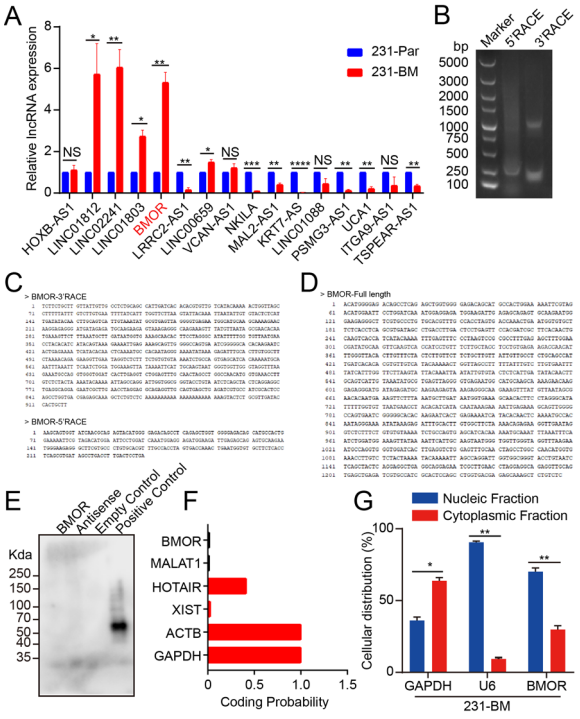

Fig. S1. LncRNA BMOR is a real lncRNA that is associated with brain metastasis. (A) RT–qPCR results show that BMOR is one of the most upregulated lncRNAs in 231-BM cells versus 231-Par cells among the selected lncRNAs. *p < 0.05, **p < 0.01, ***p < 0.001, ****p < 0.0001, NS for not significant (t test). (B) A representative image of the 2D gel electrophoresis experiment in the 5' and 3' RACE assays. (C) The sequence of BMOR identified by 3' and 5' RACE. (D) The sequence of the full-length BMOR. (E) An in vitro transcription/translation assay showed that BMOR has no detectable polypeptide products. BMOR: full-length BMOR; Antisense: antisense of full-length BMOR; Empty control: empty vector of PCDNA3.1 served as a negative control; Positive control: PCDNA3.1 with luciferase gene used as a positive control. (F) In silico analysis of the full-length BMOR sequence reveals BMOR without any coding probability using the web server for Coding Potential Assessing Tool (CPAT) (http://lilab.research.bcm.edu/). (G) Subcellular fractionation analysis revealed that BMOR was predominantly distributed in the nucleic fraction versus the cytoplasmic fraction in 231-BM cells using RT–qPCR. GAPDH and U6 were used as cytoplasmic and nucleic fraction markers, respectively. *p < 0.05, **p < 0.01 (t test).

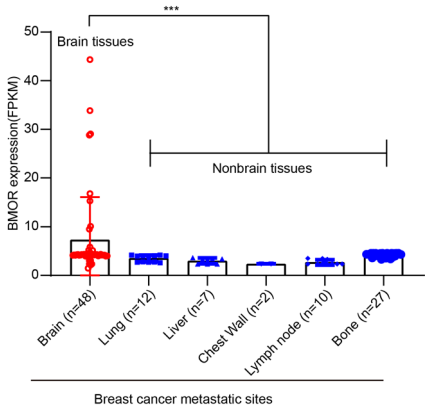

Fig. S2. Analysis of BMOR expression in metastatic breast cancers using data archived in the human cancer metastasis database (HCMDB) reveals that BMOR only shows substantially high expression in breast cancer metastasis to brain tissue as compared with breast cancer metastasis to nonbrain tissues, including lung, liver, chest wall, lymph node, and bone. *** $p < 0.001$ (t test).

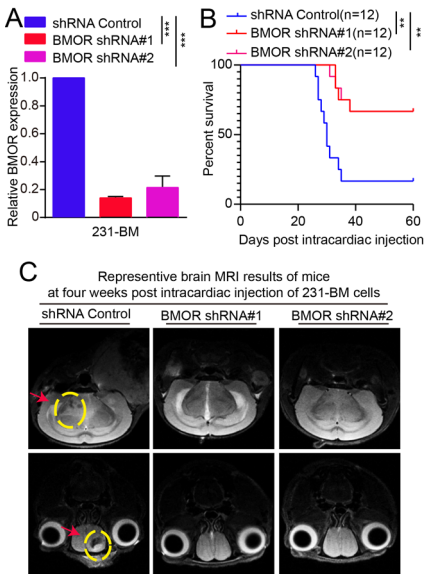

Fig. S3. Depletion of BMOR in 231-BM cells by BMOR shRNAs versus control significantly suppresses the formation of metastatic lesions in brain metastases in an intracardiac injection nude mouse model. (A) RT–qPCR confirmed that BMOR expression was successfully depleted in 231-BM cells using BMOR shRNA#1 and BMOR shRNA#2 compared with the scrambled shRNA control. ***p < 0.001(t test). (B-C) Another set of female immunodeficient mice undergoing intracardiac injection of 231-BM cells with versus without BMOR depletion shows that BMOR promotes brain metastasis. (B) Overall survival analysis of mice reveals that the recipient mice bearing BMOR-depleted 231-BM cells versus controls show longer survival times. Log rank test: p = 0.0024 for shRNA Control vs. BMOR shRNA#1 and p = 0.0023 for shRNA Control vs. BMOR shRNA#2. **p < 0.01. (C) Presentative images of brain metastases in mice using MRI Imaging System show that depletion of BMOR in 231-BM cells inhibits the formation of metastatic lesions in the mouse brain. The metastatic lesions in the brain are indicated by dashed yellow circles with red arrows.

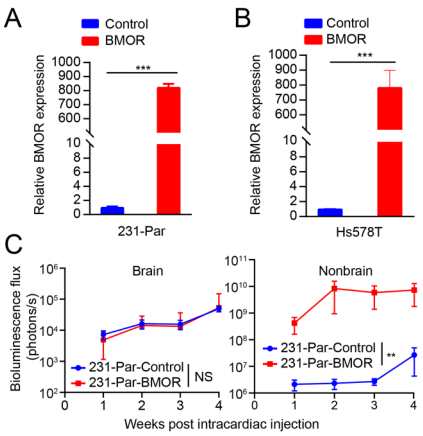

Fig. S4. The impacts of BMOR overexpression on brain metastasis development. (A) RT–qPCR analysis confirmed successful overexpression of BMOR in 231-Par cells using PLV-luci-BMOR (BMOR) compare with the control using PLV-luci-control (Control). ***$p < 0.001$ (t test). (B) RT–qPCR analysis confirmed successful overexpression of BMOR in Hs578T cells using PLV-luci-BMOR (BMOR) compared with the control using PLV-luci-control (Control). ***$p < 0.001$ (t test). (C) Quantification of bioluminescence flux in brain (left) and nonbrain (right) tissue on the data from IVIS Imaging System with indicated treatment across time. The results show that intracardiac injection of BMOR-overexpressing 231-Par cells versus control cells cannot enhance the formation of metastatic tumors in the mouse brain. **$p < 0.01$, NS for not significant (t test).

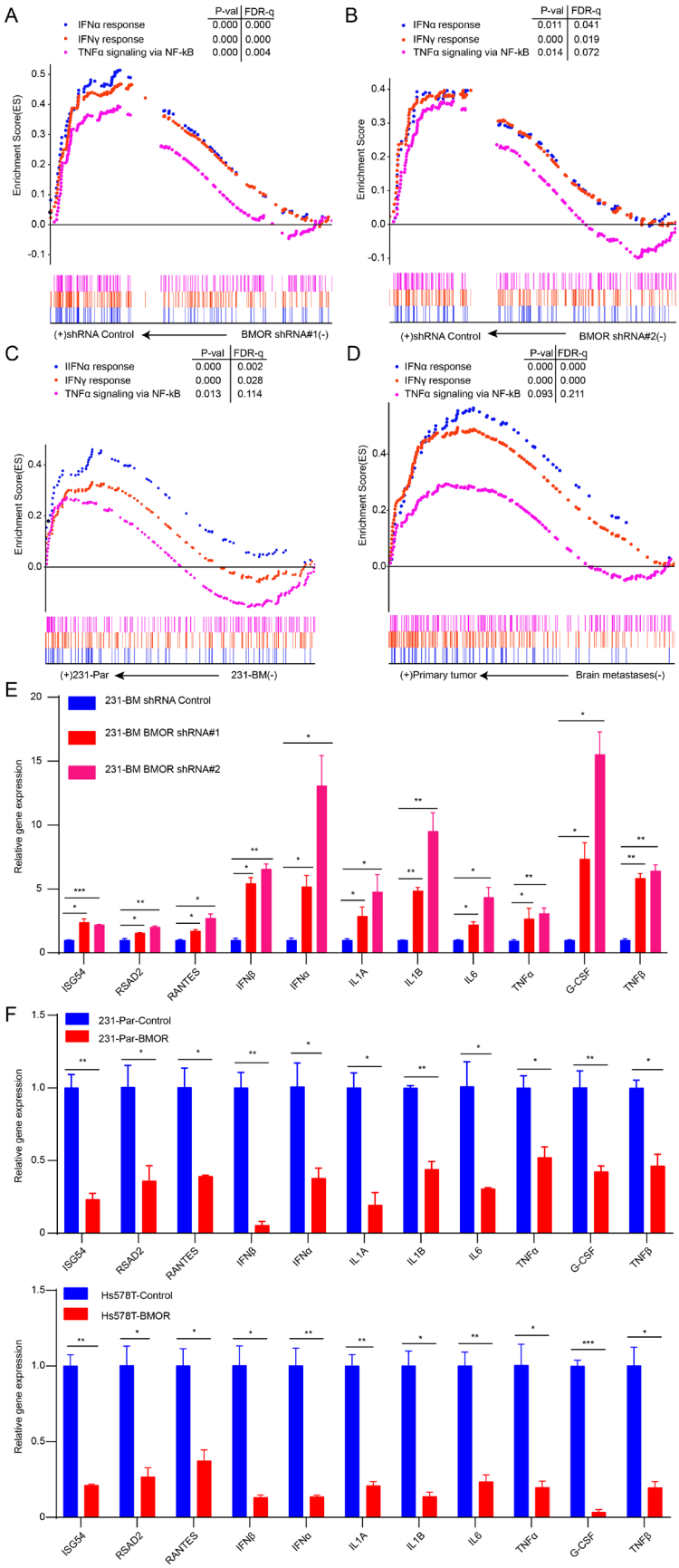
A
IFNα response
IFNγ response
TNFα signaling via NF-kB
P-val FDR-q
0.000 0.000
0.000 0.000
0.000 0.004
Enrichment Score(ES)
(+)shRNA Control
BMOR shRNA#1(-)
B
IFNα response
IFNγ response
TNFα signaling via NF-kB
P-val FDR-q
0.011 0.041
0.000 0.019
0.014 0.072
Enrichment Score
(+)shRNA Control
BMOR shRNA#2(-)
C
IIFNα response
IFNγ response
TNFα signaling via NF-kB
P-val FDR-q
0.000 0.002
0.000 0.028
0.013 0.114
Enrichment Score(ES)
(+)231-Par
231-BM(-)
D
IFNα response
IFNγ response
TNFα signaling via NF-kB
P-val FDR-q
0.000 0.000
0.000 0.000
0.093 0.211
Enrichment Score(ES)
(+)Primary tumor
Brain metastases(-)
E
231-BM shRNA Control
231-BM BMOR shRNA#1
231-BM BMOR shRNA#2
Relative gene expression
ISG54
RSAD2
RANTES
IFNβ
IFNα
IL1A
IL1B
IL6
TNFα
G-CSF
TNFβ
F
231-Par-Control
231-Par-BMOR
Relative gene expression
Hs578T-Control
Hs578T-BMOR
Relative gene expression

Fig. S5. BMOR inhibits several immune response pathways important for inducing cytotoxicity of cancer cells. (A-D) Gene Set Enrichment Analysis (GSEA) shows that BMOR inhibits several immune response pathways important for inducing the cytotoxicity of cancer cells, including IFNα and IFNγ responses and TNFα signaling via NF-κB. "(+)" and "(-)", respectively, indicate upregulation and downregulation of immune response pathways. (A-B) GSEA transcriptome analysis of 231-BM cells with depletion of BMOR versus control showed upregulation of IFNα and IFNγ responses and TNFα signaling via NF-κB. (C) GSEA transcriptome analysis of 231-BM cells compared with 231-Par cells revealed downregulation of IFNα and IFNγ responses and TNFα signaling via NF-κB. (D) GSEA transcriptome analysis of brain metastases versus their matched primary breast tumors revealed downregulation of IFNα and IFNγ responses and TNFα signaling via NF-κB. Data were retrieved from a publicly available dataset: GEO GSE125989. (E-F) BMOR inhibits the expression of ISGs, IFNs, and cytokine genes associated with the immune response pathways important for inducing cytotoxicity of cancer cells, including ISG54, RSAD2, RANTES, IFNβ, IFNα, IL1A, IL1B, IL6, TNFα, G-CSF and TNFβ. Individual genes are indicated with gene names. (E) RT-qPCR results show that depletion of BMOR in 231-BM versus controls upregulates the expression of ISG54, RSAD2, RANTES, IFNβ, IFNα, IL1A, IL1B, IL6, TNFα, G-CSF and TNFβ. *$p < 0.05$, **$p < 0.01$, ***$p < 0.001$ (t test). (F) RT–qPCR results show that overexpression of BMOR in both 231-Par and Hs578T cells versus their corresponding controls downregulates the expression of ISG54, RSAD2, RANTES, IFNβ, IFNα, IL1A, IL1B, IL6, TNFα, G-CSF and TNFβ. *$p < 0.05$, **$p < 0.01$, ***$p < 0.001$ (t test).

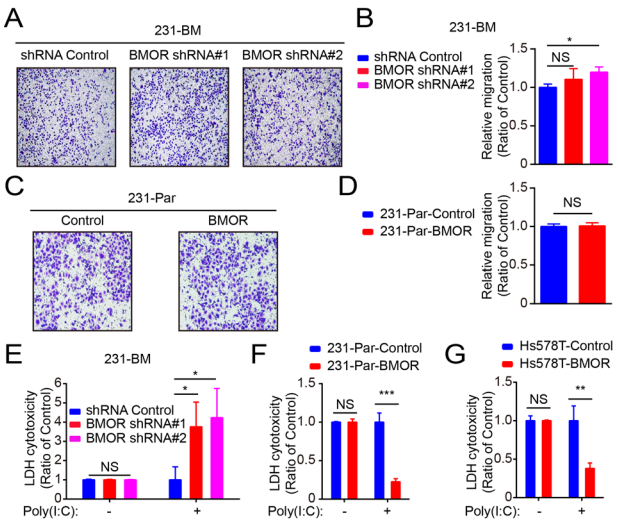

Fig. S6. Effects of BMOR on the migration potential and cytotoxicity of cancer cells. (A-D) BMOR cannot enhance the migration potential of cancer cells in migration and invasion assays in in vitro cancer cell culture without additional treatment. (A-B) Migration and invasion assays show that BMOR depletion versus control does not reduce the migration potential of 231-BM cells: (A) Representative images; (B) Quantification. *p < 0.05, NS for not significant (t test). (C-D) Migration and invasion assays show that BMOR overexpression versus control does not enhance the migration potential of 231-Par cells: (C) Representative images; (D) Quantification. NS for not significant (t test). (E-G) BMOR inhibits the Poly(I:C)-induced cytotoxicity of cancer cells in LDH cytotoxicity assays. (E) The results of LDH cytotoxicity assays show that upon Poly(I:C) treatment but not without, BMOR depletion versus control increases the cytotoxicity of 231-BM cells. *p < 0.05, NS for not significant (t test). (F) The results of LDH cytotoxicity assays show that upon Poly(I:C) treatment but not without, BMOR overexpression versus control decreases the cytotoxicity of 231-Par cells. ***p < 0.001, NS for not significant (t test). (G) The results of LDH cytotoxicity assays show that upon Poly(I:C) treatment but not without, BMOR overexpression versus control decreases the cytotoxicity of Hs578T cells. **p < 0.01, NS for not significant (t test).

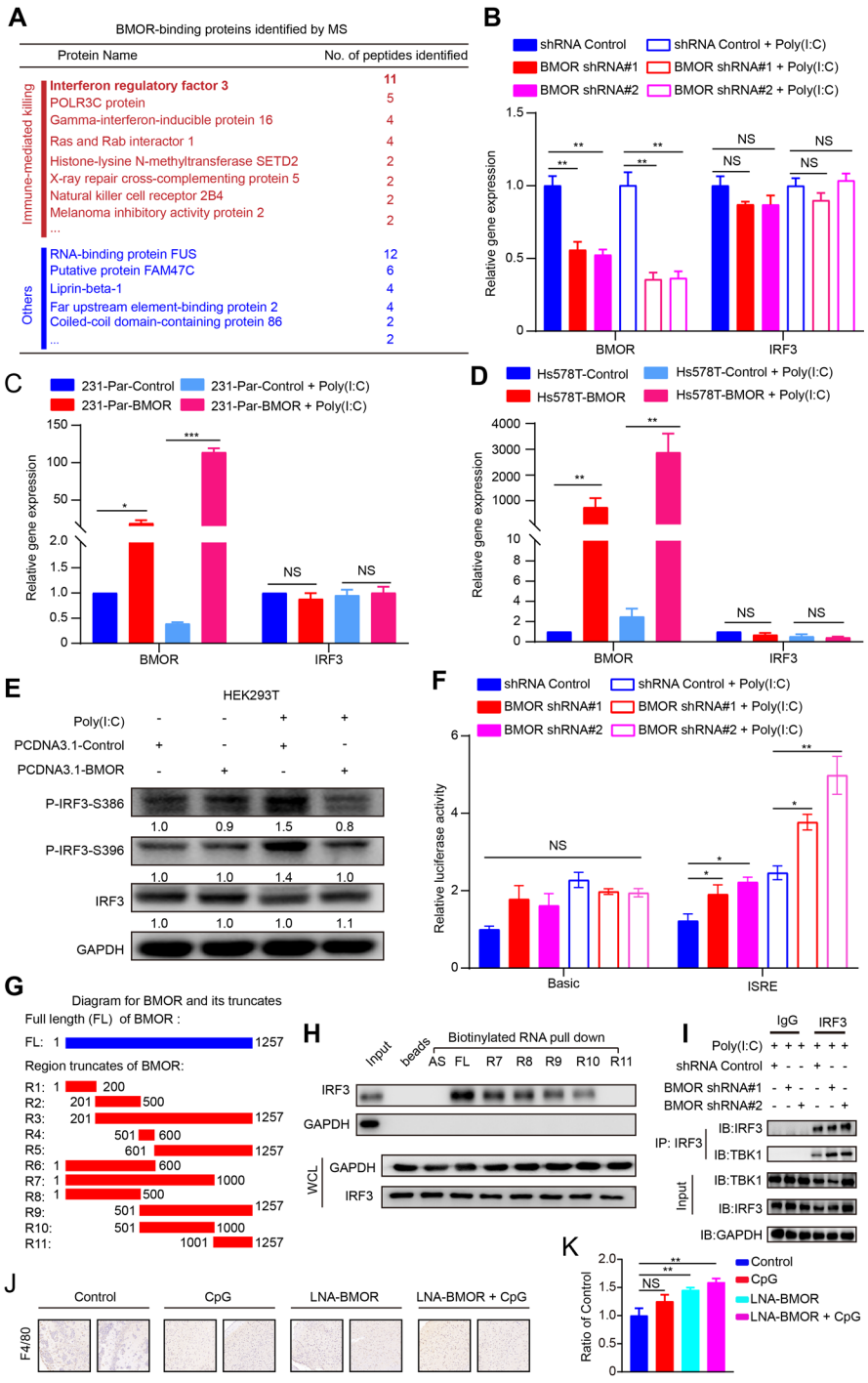

Fig. S7. Brain-enriched lncRNA BMOR binds IRF3 and inhibits IRF3 phosphorylation and activation in cells. (A) Selected BMOR-binding proteins identified by RNA pull down-MS from Dataset 6. (B-D) Modulation of BMOR expression does not affect the mRNA expression level of IRF3. (B) RT–qPCR results show that with or without Poly(I:C) treatment, depletion of BMOR in 231-BM cells versus the corresponding controls cannot significantly affect the expression of the IRF3 gene. **p < 0.01, NS for not significant (t test). (C) RT–qPCR results show that with or without Poly(I:C) treatment, overexpression of BMOR in 231-Par cells versus the corresponding controls cannot significantly affect the expression of the IRF3 gene. *p < 0.05, ***p < 0.001, NS for not significant (t

test). (D) RT–qPCR results show that with or without Poly(I:C) treatment, overexpression of BMOR in Hs578T cells versus the corresponding controls cannot significantly affect the expression of the IRF3 gene. **p < 0.01, NS for not significant (t test). (E) In HEK293T cells, representative western blot images show that overexpression of BMOR as compared to control can reduce the phosphorylation level of IRF3 but not the protein level of IRF3. (F) The results of luciferase reporter assays show that with or without Poly(I:C) treatment, depletion of BMOR in 231-BM cells versus the corresponding controls significantly increased the luciferase activity of the ISRE-containing promoter. *p < 0.05, **p < 0.01, NS for not significant (t test). (G) A diagram of BMOR and its truncation deletions, including those used in Fig. 4G and Fig. S7H for BMOR-IRF3 domain mapping assays. (H) A representative western blot image of biotinylated RNA pull down assays performed to map the IFR3-binding region in BMOR required for interaction with IRF3: FL and AS represent full-length BMOR and its antisense, respectively. The results support that the IBR1 (1-200 bp) and IBR2 (500-600 bp) regions in BMOR are critical for the BMOR-IRF3 interaction. (I) Representative western blot images of Co-IP assays show that depletion of BMOR in 231-BM cells versus control cells increases TBK1 coprecipitation with IRF3. (J-K) The results of immunohistochemical staining using an antibody for F4/80 (a well-characterized microglial marker) show that LNA-BMOR and CpG treatment compared with control can increase the recruitment of microglia in the brain metastatic lesions. (J) Representative immunohistochemical staining images (200 ×) using antibodies for F4/80 protein with the indicated treatments. (K) Quantification of immunohistochemical staining images. *p < 0.05, **p < 0.01, NS for not significant (t test).

Table S1. Primers used for RT-qPCR.

Gene name	Forward primer sequence	Reverse primer sequence
GAPDH	AGCCACATCGCTCAGACAC	GCCCAATACGACCAAATCC
U6	GCTTGCTTCAGCAGCACATA	AAAAACATGGAACTCTTCACG
BMOR	GAGTTCCACGATCGCTTCAC	GTGATCAATGGCTGCAGAGG
HOXB-AS1	GGGACTCCAGCGAAATTACA	AGGCACTGGTGTAGGAATGG
LINC01812	GTGAAGAGCACTGTGGGTGA	GGCCTTCCTGAGTTCCTCTT
LINC02241	CATGGGGTCGTCTTCATCCC	CAGAACCCTTTGTCCACGGT
LINC01803	GGCACCTGGATTAAGCAGAC	GGGATGTAGACCAGCCTCTG
LRRC2-AS1	TCAGCCCATCAGATAGCAGC	GGATGATGCGTAGCGTTCCT
LINC00659	AGAGCATGTTTTCCTTGGCTTT	TATGTCAGCTGTGATGTGGCA
VCAN-AS1	AGAGCATGTTTTCCTTGGCTTT	TATGTCAGCTGTGATGTGGCA
ITGA9-AS1	GAAAGCGAAACCGTGGATAA	GCTGTGTCCACTTGCTCCTT
NKILA	CTGGTTTCGCAGGAGACTGT	CTACGCGAGTTCCCGTCTTT
MAL2-AS1	GCTAGGAACACACTCCGGTC	TGGTACTAGGTGGTGGGTGT
KRT7-AS	CTTGGCACGAGCATCCTTGA	CTCTGGTACTTGGGGGAGTAG
LINC01088	GCTGGCAGAGAGGAAGCTAA	TTAAGGGCCAGCTTGACTGT
PSMG3-AS1	CTGAACTGCCGTGTTTTGGG	GAGCGGAGACTCCATTAGCC
UCA1	CCCTACCCCAGTAATCCCCA	AGACTGCCTTTGGGTTGAGG
TSPEAR-AS1	CTGAAGCAACATCAGGCGGA	AAAACACGGGGCTTCTGTCA
MALAT1	ATTGCCGACCTCACGGATTT	CAGCAGCAGACAGGATTCCA
IL1A	TGGTAGTAGCAACCAACGGGA	ACTTTGATTGAGGGCGTCATTC
IL1B	AGCTACGAATCTCCGACCAC	CGTTATCCCATGTGTCGAAGAA
IL6	ACTCACCTCTTCAGAACGAATTG	CCATCTTTGGAAGGTTCAGGTTG
TNFα	CCTCTCTCTAATCAGCCCTCTG	GAGGACCTGGGAGTAGATGAG
G-CSF	GCTGCTTGAGCCAACTCCATA	GAACGCGGTACGACACCTC
IFNα	GCCTCGCCCTTTGCTTTACT	CTGTGGGTCTCAGGGAGATCA
IFNβ	GCTTGGATTCCTACAAAGAAGCA	ATAGATGGTCAATGCGGCGTC
TNFβ	ATGACACCACCTGAACGTCTC	CTCTCCAGAGCAGTGAGTTCT
RANTES	CCAGCAGTCGTCTTTGTCAC	CTCTGGGTTGGCACACACTT
ISG54	AAGCACCTCAAAGGGCAAAAC	TCGGCCCATGTGATAGTAGAC
RSAD2	TGGGTGCTTACACCTGCTG	GAAGTGATAGTTGACGCTGGTT

Table S2. Primers used for 5’ and 3’ RACE of BMOR.

RACE type	Primer sequence
5’ RACE	outer primer: GCAGAGGCAACAATAACAAGCAGAAGAA inner primer: TCAGGAGTCAAGGTCAGGCTATCACGCT
3’ RACE	outer primer: GGATCAAATGGAGGAGATGGAAG inner primer: TCTTCTGCTTGTTATTGTTGCCTC

Table S3. Primers used for generation vectors for transfection of cells.

Plasmid name	Forward primer sequence	Reverse primer sequence
PCDNA3.1-BMOR-FL	CTAGCTAGCACATGGGGAGACAG CCTCAGAGCTGGT	CCCAAGCTTGAGACAGAGCTTTGCTCT CGTCACCAG
PCDNA3.1-BMOR-R1	CTAGCTAGCACATGGGGAGACAG CCTCAGAGCTGGT	CCCAAGCTTGCTATCACGCTGAGGTGA GAAGCACAC
PCDNA3.1-BMOR-R2	CTAGCTAGCCTGACCTTGACTCCT GAGTTCCACGAT	CCCAAGCTTTACTTAAGAACCAAATGAT AAAATTCA
PCDNA3.1-BMOR-R3	CTAGCTAGCCTGACCTTGACTCCT GAGTTCCACGAT	CCCAAGCTTGAGACAGAGCTTTGCTCT CGTCACCAG
PCDNA3.1-BMOR-R4	CTAGCTAGCTTACAAATTAATATTG TGTACTCTCAT	CCCAAGCTTCTTGTTCTTTTGCTTGCAT GCCATTCT
PCDNA3.1-BMOR-R5	CTAGCTAGCGAGAGGGATGATAGA GATGCAAGAAGA	CCCAAGCTTGAGACAGAGCTTTGCTCT CGTCACCAG
PCDNA3.1-BMOR-R6	CTAGCTAGCACATGGGGAGACAG CCTCAGAGCTGGT	CCCAAGCTTCTTGTTCTTTTGCTTGCAT GCCATTCT
PCDNA3.1-BMOR-R7	CTAGCTAGCACATGGGGAGACAG CCTCAGAGCTGGT	CCCAAGCTTCCCATTACTTGCAATGAAT TTTATAAC
PCDNA3.1-BMOR-R8	CTAGCTAGCACATGGGGAGACAG CCTCAGAGCTGGT	CCCAAGCTTTACTTAAGAACCAAATGAT AAAATTCA
PCDNA3.1-BMOR-R9	CTAGCTAGCTTACAAATTAATATTG TGTACTCTCAT	CCCAAGCTTGAGACAGAGCTTTGCTCT CGTCACCAG
PCDNA3.1-BMOR-R10	CTAGCTAGCTTACAAATTAATATTG TGTACTCTCAT	CCCAAGCTTCCCATTACTTGCAATGAAT TTTATAAC
PCDNA3.1-BMOR-R11	CTAGCTAGCTGGTTGGGTAGGTTT AAGAAATGCCAG	CCCAAGCTTGAGACAGAGCTTTGCTCT CGTCACCAG
P3×Flag-CMV-IRF3	CCCAAGCTTATGGGAACCCCAAA GCCACGGATCCTG	CCGGAATTCTCAGCTCTCCCCAGGGC CCTGGAAATC
P3×Flag-CMV-IRF3-K1	CCCAAGCTTATGGGAACCCCAAA GCCACGGATCCTG	CCGGAATTCTCACCCTACCCGGGCCAT TTCTACCAA
P3×Flag-CMV-IRF3-K2	CCCAAGCTTATGGGAACCCCAAA GCCACGGATCCTG	CCGGAATTCTCACAGAATGTCTTCCTG GGTATCAGA
P3×Flag-CMV-IRF3-K3	CCCAAGCTTGATGAGTTACTGGGT AACATGGTGTTG	CCGGAATTCTCAGCTCTCCCCAGGGC CCTGGAAATC
P3×Flag-CMV-IRF3-K4	CCCAAGCTTGAGTGGGAGTTCGA GGTGACAGCCTTC	CCGGAATTCTCAGCTCTCCCCAGGGC CCTGGAAATC
P3×Flag-CMV-IRF3-K5	CCCAAGCTTATGGGAACCCCAAA GCCACGGATCCTG	CCGGAATTCTTCCCCCGGCACCAACA GCCGCTTCAG
P3×Flag-CMV-IRF3-K6	CCCAAGCTTGATGAGTTACTGGGT AACATGGTGTTG	CCGGAATTCTCACCCTACCCGGGCCAT TTCTACCAA
pLV-Luci-BMOR	CCGCTCGAGACATGGGGAGACAG CCTCAGAGCTGGT	CGCGGATCCGAGACAGAGCTTTGCTC TCGTCACCAG
pLKO.1-BMORshRNA#1	CCGGACTTGCAGTCATTGTAAATA TCTCGAGATATTTACAATGACTGCA AGTTTTTTG	AATTCAAAAAACTTGCAGTCATTGTAAA TATCTCGAGATATTTACAATGACTGCAA GT
pLKO.1-BMOR shRNA #2	CCGGACCTACACATCATACAATAA ACTCGAGTTTATTGTATGATGTGTA GGTTTTTTG	AATTCAAAAAACCTACACATCATACAAT AAACTCGAGTTTATTGTATGATGTGTAG GT
PGL3-ISRE-Luci	CGGGAAAGTGAAACTAGGGAAAG TGAAACTAGGGAAAGTGAAACTAA	GATCTTAGTTTCACTTTCCCTAGTTTCA CTTTCCCTAGTTTCACTTTCCCGGTAC

Dataset S1. (separate file). Transcription profiles of 231-BM cells vs. 231-Par cells.

Dataset S2. (separate file). Transcription profiles of 231-BM cells with vs. without BMOR depletion.

Dataset S3. (separate file). List of altered GSEA pathways in BMOR-depleted 231-BM cells compared to 231-BM cells without BMOR depletion.

Dataset S4. (separate file). List of altered GSEA pathways in 231-BM cells compared to 231-Par cells.

Dataset S5. (separate file). List of altered GSEA pathways in brain metastases compared to their paired primary breast tumors.

Dataset S6. (separate file). List of BMOR-binding proteins identified by RNA pull down-MS.